



Effects of Increasing Drag on Conjunction Assessment

Ryan Clayton Frigm¹ and David P. McKinley²
a.i. solutions, Inc., Lanham, MD, 20706

Conjunction Assessment Risk Analysis relies heavily on the computation of the Probability of Collision (Pc) and the understanding of the sensitivity of this calculation to the position errors as defined by the covariance. In Low Earth Orbit (LEO), covariance is predominantly driven by perturbations due to atmospheric drag. This paper describes the effects of increasing atmospheric drag through Solar Cycle 24 on Pc calculations. The process of determining these effects is found through analyzing solar flux predictions on Energy Dissipation Rate (EDR), historical relationship between EDR and covariance, and the sensitivity of Pc to covariance. It is discovered that while all LEO satellites will be affected by the increase in solar activity, the relative effect is more significant in the LEO regime around 700 kilometers in altitude compared to 400 kilometers. Furthermore, it is shown that higher Pc values can be expected at larger close approach miss distances. Understanding these counter-intuitive results is important to setting Owner/Operator expectations concerning conjunctions as solar maximum approaches.

I. Introduction

CONJUNCTION assessment risk analysis (CARA) is the process of quantifying the risk associated with any identified close approaches between two orbiting objects. NASA Goddard Space Flight Center (GSFC) has implemented a routine CARA process that currently supports approximately 55 robotic spacecraft [References 1,2]. Often the collision risk associated with a conjunction is quantified in the form of the Probability of Collision, Pc. The computation of Pc requires both state and uncertainty information of the two conjuncting objects. The uncertainty information is provided in the form of a covariance. In Low Earth Orbiting (LEO), satellite covariance is predominantly driven by perturbations due to atmospheric drag. It is also well-known that atmospheric drag is a dynamic effect dictated by solar activity. This analysis seeks to understand the effects of increasing atmospheric drag on CARA through analysis of the Pc calculation.

II. Background

The typical method for computing the Pc for a high relative velocity encounter is given by Reference 1. With the assumption of a high relative velocity encounter, the problem is reduced to a two-dimensional conjunction plane constructed at the Time of Closest Approach (TCA) between the two spacecraft as shown in Figure 1. One object is located at the origin of the conjunction plane while the other is offset by the miss distance, R_m , along the x-axis. The physical sizes of the spacecraft involved are represented by a spherical volume, V , centered on the second object. The full three dimensional combined position uncertainties of both objects is given by the covariance matrix C , which is projected into the conjunction plane as C^* .

¹ Mission Analyst, Mission Services Division, AIAA Member

² Project Engineer, Mission Services Division, AIAA Senior Member

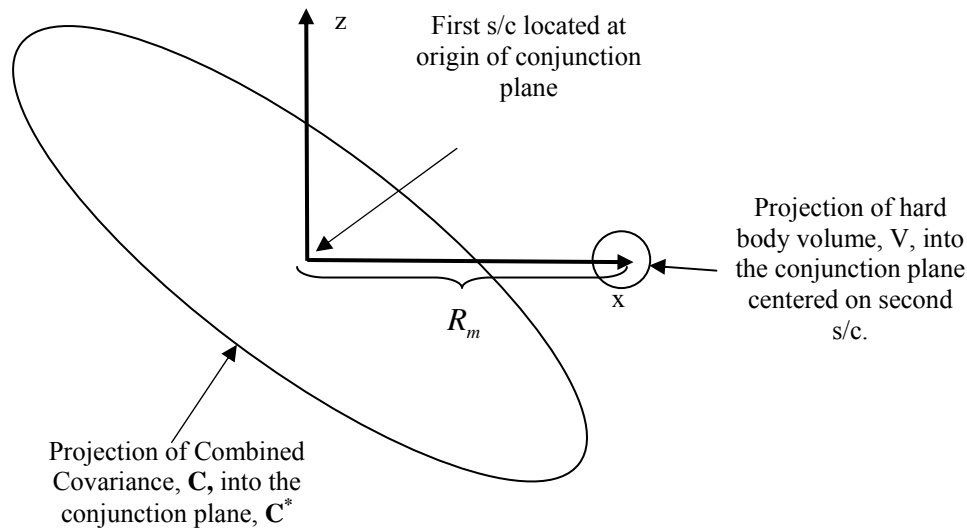


Figure 1. Conjunction Plane Geometry

Given the geometry of the conjunction, the P_c [Reference 3] can then be calculated as

$$P_c = \frac{1}{\sqrt{(2\pi)^2 |\mathbf{C}^*|}} \iint_A e^{-\frac{1}{2} \vec{r}^T \mathbf{C}^{*-1} \vec{r}} dx dz \quad (1)$$

where $\vec{r} = \begin{Bmatrix} x \\ z \end{Bmatrix}$ coordinates in the conjunction plane and A is the projection of volume V onto the plane.

For any given close approach geometry (*i.e.* miss distance vector), Equation 1 can be integrated over a range of covariance sizes to produce a distinctive curve such as the one shown in Figure 2. This is a key assumption: regardless of miss distance, a range of covariance can be found such that P_c curve exhibits the behavior shown in Figure 2. The P_c is plotted versus a single Scale Factor (SF) which directly multiplies the covariance in Equation 1, effectively scaling the full covariance. The typical behavior of the P_c as SF increases is to gradually increase to a maximum P_c , followed by a steep drop off. Obviously, to the left of the maximum P_c , the P_c is more sensitive than to the right of that maximum P_c . Likewise, if the covariance is held constant and the miss distance is varied, a similar trend will be produced highlighting that the P_c can be parameterized as a ratio between the covariance size and the miss distance.

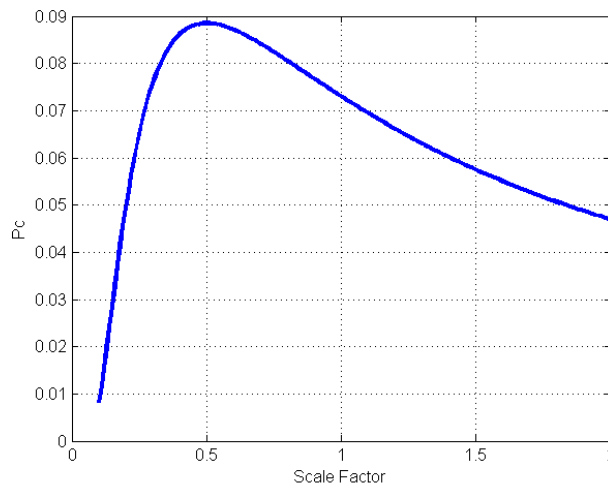


Figure 2. Probability of Collision as a Function of Scale Factor.

Many factors go into the size of the covariance resulting from an orbit determination (OD) solution and will determine where on the Pc curve shown in Figure 2 a given solution will lie. The type, quantity, and quality of measurements, accuracy of the force models, and in some cases the processing algorithm (i.e. Kalman Filter, Batch Processor, Unscented Filter) will determine the epoch accuracy of a given covariance. To calculate Pc for predicted conjunction events, the covariance must be propagated from the OD solution epoch to the TCA. The magnitude of the propagated covariance depends on the magnitude of the epoch covariance (and hence all of its contributors) as well as the accuracy of the propagation force models and the inclusion of process noise.

It is well known and understood that for LEO spacecraft one of the primary perturbing forces is atmospheric drag. It is also well known that atmospheric drag is one of the most difficult forces to predict accurately. Therefore, uncertainty in atmospheric drag is a major contributor to the size of a predicted covariance. To date, the GSFC CARA team's experience perform Pc analysis has been limited to a quiet period of solar activity, resulting in the vast majority of conjunctions analyzed being on the left, or steep gradient, side of the Pc curve. This situation typically ensures that Probabilities fall off quickly, even for small miss distances.

Now that we are beginning another solar cycle, and atmospheric drag is predicted to increase, it is beneficial to determine the impact on the typical conjunction encountered. Given that Pc can be parameterized as a ratio between the miss distance and covariance size, as covariance size grows due to the increased uncertainty in atmospheric drag, it is hypothesized that higher probabilities may be observed at larger miss distances. Likewise, probabilities at relatively smaller miss distances may be observed to decrease. Understanding these impacts is critical to informing mission operators of the appropriate conjunction risks. In the next sections, the analysis will attempt to parameterize covariance size as a function of drag from an historical data set and then use these findings to determine expected changes in analyzing typical conjunctions.

III. Historical Covariance versus Energy Dissipation Rate Trends

The atmospheric drag force imparted on a spacecraft is due to the spacecraft physical properties such as frontal area and mass, the atmospheric density, and the orbital velocity of the spacecraft. A suitable parameterization of the effect of drag on a given spacecraft is the Energy Dissipation Rate (EDR) due to atmospheric drag, which is defined as the dot product between the drag acceleration vector and the orbital velocity:

$$EDR = \vec{a}_D \cdot \vec{V} \quad (2)$$

The drag acceleration vector is a function of the atmospheric density ρ , drag coefficient C_D , spacecraft mass m , frontal area A , and velocity V

$$\vec{a}_D = -\frac{1}{2}\rho C_D \frac{A}{m} V^2 \hat{V} \quad (3)$$

Combining the drag coefficient, area, and mass into a single ballistic coefficient β and assuming that the orbit is circular, Equations 2 and 3 can then be combined to show that EDR is a function of the atmospheric density, ballistic coefficient, and spacecraft semi-major axis.

$$EDR = -\frac{1}{2}\rho\beta\left(\frac{\mu}{a^3}\right)^{3/2} \quad (4)$$

EDR will be used from here on to characterize the amount of drag acting on a spacecraft.

The existing set of missions supported by the GSFC CARA Team includes missions spanning from the Tropical Rainfall Measurement Mission (TRMM) at approximately 400 kilometers altitude, the Earth Science Constellation (ESC) missions at approximately 700 km altitude, and the Jason-1, Jason-2, and TOPEX/Poseidon missions at approximately 1300 km altitude. Even during the low solar flux environment of the past five years, this wide range of altitudes gives a useful set of data to parameterize covariance as a function of EDR. Figure 3 plots the observed normalized covariance size versus EDR for a range of propagation times. The metric chosen to represent covariance

magnitude is the RSS of the diagonal of the covariance matrix in the Radial, In-Track, and Cross-Track (RIC) coordinate system.

The intent is to investigate the change in covariance due only to EDR differences. Therefore, an effort was made to control other variables which influence covariance. The data set used to produce Figure 3 represents well-tracked objects with similar tracking data density and quality.

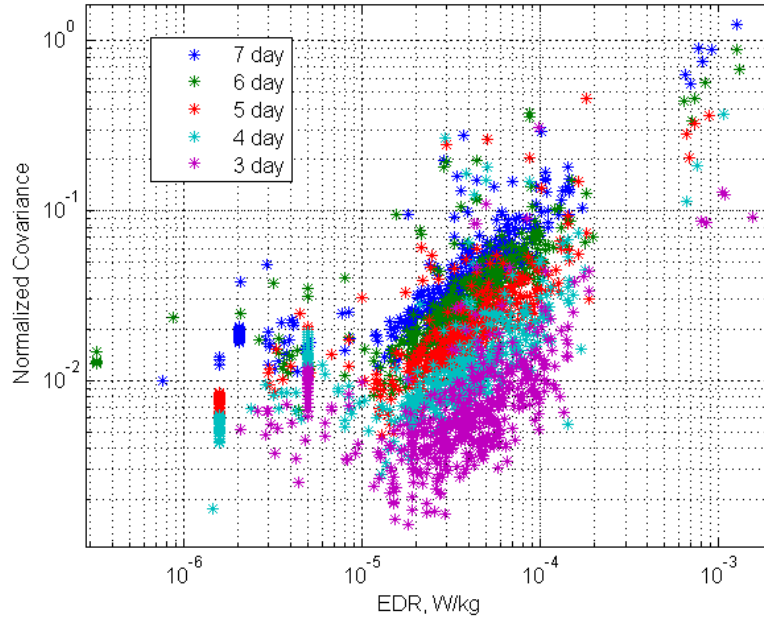


Figure 3. Normalized Covariance versus EDR for Various Propagation Durations.

The correlation between covariance size and propagation time is evident from Figure 3. In an attempt to determine the correlation between EDR and the normalized covariance, the data for seven and three day propagation times are given in Figures 4 and 5. In these data sets, points that could be identified as outliers were removed. Outliers consisted of orbit determination solutions that occurred just after spacecraft maneuvers when the post maneuver orbit had not been fully resolved. It is noted that for both data sets there are significant gaps in the data and that the data is extremely sparse at high EDR values. For these sparse data sets, a linear fit was performed resulting in the relationships

$$COV = 1.3e3EDR + 0.01 \text{ (7 Day)} \quad (5)$$

$$COV = 91EDR + 0.005 \text{ (3 Day)} \quad (6)$$

The seven day fit showed an R-squared fit value of around 0.9. The three day fit showed a fit value of 0.8. The quality of these fits is driven primarily by the lack of data at the high EDR values. In fact, Figure 5 suggests that there may be considerable variation in covariance at large values of EDR. The correlation between EDR and Covariance size will require additional analysis to confirm this correlation as more high drag data becomes available. However, since the goal of this analysis is to bound the expected behavior of the covariance and ultimately the probability of collision, rather than accurate prediction of these values, we will assume these linear relationships for the remainder of this analysis.

The slope of the curve fit demonstrates a dependence on the propagation duration. This is expected since uncertainty typically increases with propagation time. Also, the y-axis intercept demonstrates a dependence on the propagation duration. In the strictest sense, the y-axis intercept should be the covariance magnitude with zero drag force, and therefore zero uncertainty due to drag. The increase in the y-intercept is also as expected given that even with no atmospheric drag, the error covariance is expected to grow over time due to other system dynamics. These

relationships will be used in later sections to estimate the expected covariance magnitude during the coming solar maximum.

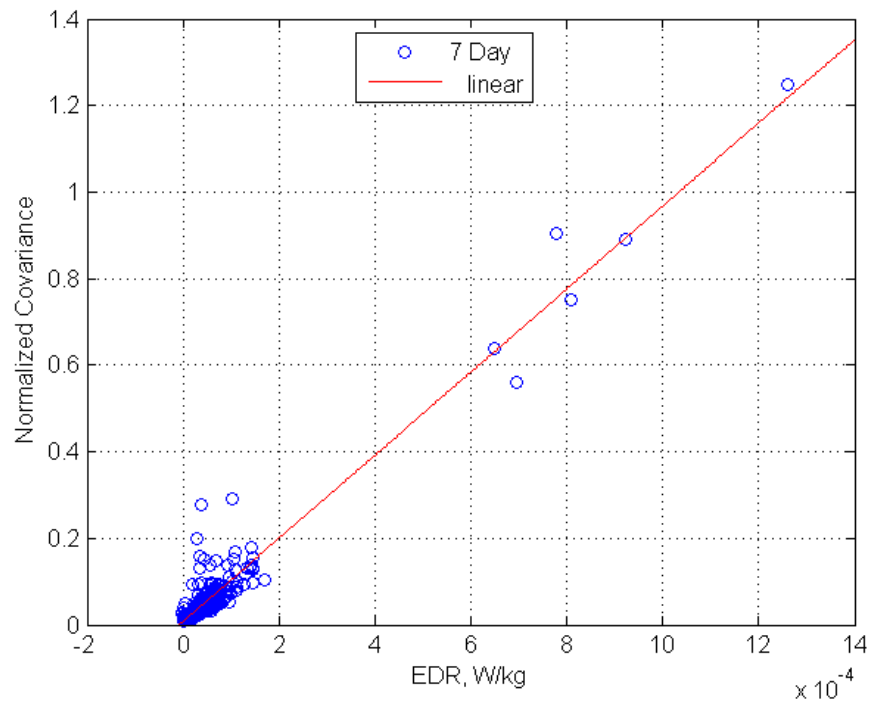


Figure 4. Normalized Covariance vs. EDR for Seven Day Propagation.

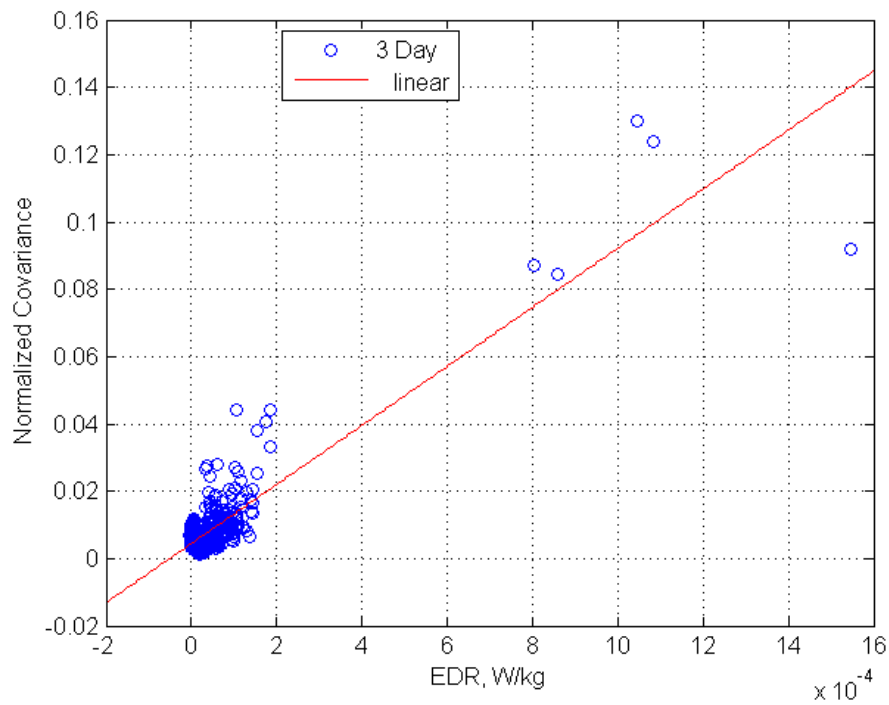


Figure 5. Normalized Covariance vs. EDR for Three Day Propagation.

IV. Expected EDR Growth during Next Solar Cycle

In order to use Equations (5) and (6) to determine the covariance magnitude, the EDR during the next solar cycle must be predicted. As seen in Equations (2) through (4), EDR is a function of the spacecraft physical properties (mass, average frontal area, ballistic coefficient) and atmospheric density. The physical properties of the spacecraft are typically well known, but long-term prediction of the atmospheric density can be problematic. Atmospheric density is driven, in part, by the Extreme Ultraviolet (EUV) flux output of the Sun, measured by the energy flux at the 10.7 cm wavelength, or F10.7 index. The sun undergoes several cyclical processes that impact its energy output. For long-range space mission analysis, we are often most concerned with the 11-year solar cycle. Predictions of the F10.7 index over the next solar cycle are performed regularly by Dr. Kenneth Schatten [Reference 4] and provided to the Flight Dynamics Facility at NASA/GSFC [Reference 5]. These predictions are used along with a Jacchia-Roberts atmospheric density model to predict atmospheric density. Figure 6 shows the latest Schatten Solar Flux predictions for the upcoming Solar Cycle 24. Curves are shown for the predicted mean averaged solar flux and plus and minus 2 sigma solar flux are shown. The plus and minus two sigma curves represent the estimated uncertainty in the predicted mean behavior and can be used statistically to bound the expected EDR. This data is for the nominal timing of the solar cycle. Predictions also exist for early and late starts to the increase in solar activity, but these predictions are not used for this study. As seen in Figure 6, the peak of the next solar cycle is expected to occur in 2013.

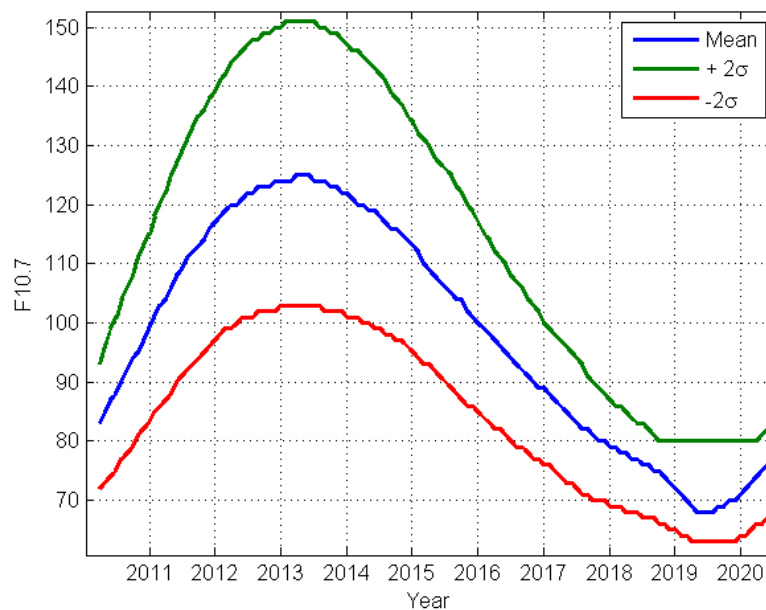


Figure 6. Schatten Solar Flux Predictions as indicated by F10.7 cm index for Solar Cycle 24.

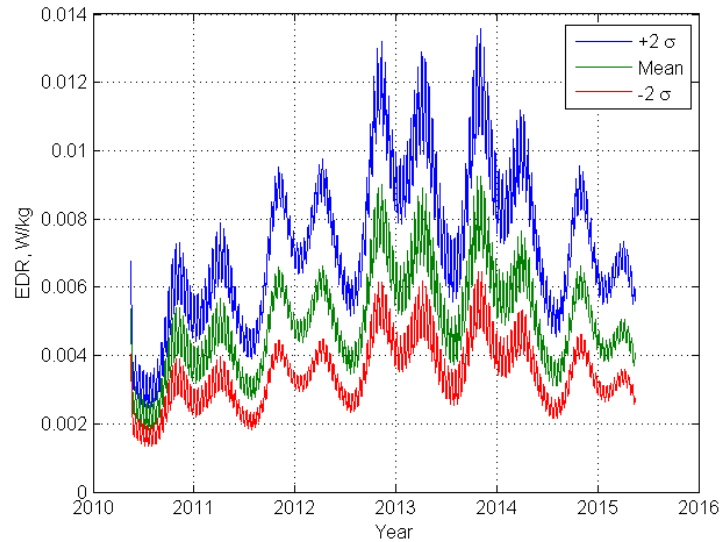
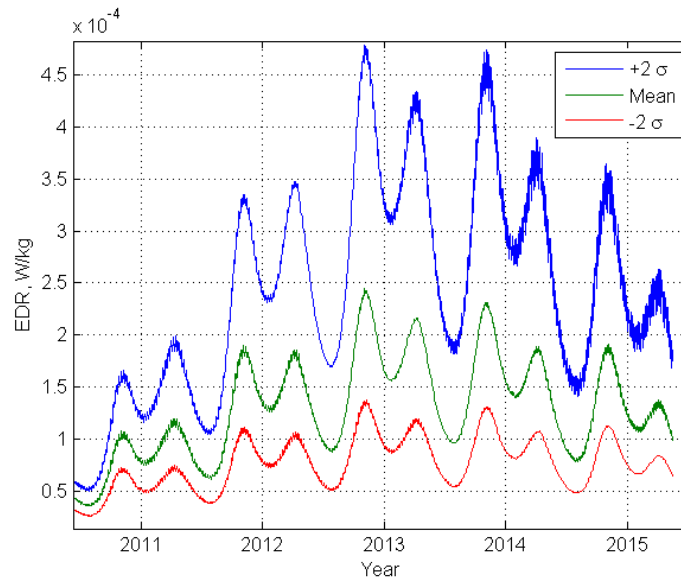
EDR predictions are made for two spacecraft. The Tropical Rainfall Measurement Mission (TRMM) is in a 400 kilometer altitude circular orbit. TRMM is one of the lowest flying spacecraft supported by the GSFC CARA Team and therefore operates at an altitude with high atmospheric density. The Earth Science Constellation (ESC) spacecraft Aqua operates in a 705 kilometer sun-synchronous orbit. Aqua operates at an altitude with a significantly less dense atmosphere than TRMM, however, the orbital regime at 700 kilometers has a very high debris density, and spacecraft in these regimes experience a significant number of conjunction events. Therefore, changes in P_c driven by increased covariance magnitude will have the largest operational impact in the ESC regime.

The physical properties for TRMM and Aqua are shown in Table 1. The frontal area and mass for each spacecraft were taken from the operational force models used to generate predicted ephemerides in the satellite Mission Operations Centers (MOC). The drag coefficient is estimated by the orbit determination process for each spacecraft. The values below represent typical values that can be expected over the next solar cycle.

Table 1. TRMM and Aqua Physical Properties.

	TRMM	Aqua
Mass, kg	2730	2800
Frontal Area, m ²	18	47
C _D	1.6	1.5

Using the physical properties in Table 1 and the Schatten Solar Flux prediction in conjunction with the Jacchia-Roberts atmosphere model predicted EDR values for TRMM and Aqua are shown in Figure 7 and Figure 8, respectively. The EDR values presented are daily averages. Periodic signatures arising from spatial and temporal variations in the atmospheric density can be seen to include long periodic seasonal dependence. As expected, the EDR peak coincides with the peak in solar flux prediction in 2013.

**Figure 7. TRMM Predicted EDR over Solar Cycle 24.****Figure 8. Aqua Predicted EDR over Solar Cycle 24.**

For TRMM, the mean profile shows an increase in EDR from 0.0028 W/kg in 2010 to 0.009 W/kg in 2013 or a 320% increase. For the plus two sigma case, a similar 320% change is observed over the same time span. For Aqua, the mean profile shows an increase from 5E-5 W/kg to 0.00024 W/kg results in a 480% increase between 2010 and 2013 and nearly 580% increase over the same time period for the plus two sigma case. For both TRMM and Aqua, the expected EDR increases from today (in low solar flux environment) to solar activity maximum. This result is straightforward – increasing atmospheric density increases the effects of drag on the spacecraft. However, the result that is counter-intuitive is the magnitude of the expected increases. The drag effects on TRMM, which resides in the higher drag environment, is expected to roughly double; whereas, Aqua is expected to be 5-8 times higher than it is today. This result is stating that the drag environment for TRMM and low altitude LEO objects is high already; however as solar activity increases, the atmosphere swells and expands in higher altitude regions and this effect is much more substantial. The result is that the increase in atmospheric density is much more profound at higher altitudes.

As a verification of this approach to predicting EDR, the starting EDR values in Figure 7 and Figure 8 were compared to observed values for TRMM and Aqua during 2010. Actual solar flux values during the first half of 2010 have fallen between the mean and minus two sigma curves of Figure 6. TRMM had an average observed EDR of 0.0015 W/kg and Aqua had an average observed EDR of 4.2e-5 W/kg showing good order of magnitude agreement between the observed and predicted EDR values, demonstrating confidence in solar flux predictions.

V. Implications on Probability of Collision Computation

To this point, this paper has described the process of predicting satellite covariance as an ultimate function of solar flux predictions. To understand how these effects on conjunction assessment, an examination of the sensitivity of the P_c to expected covariance was performed. As described in Section II, the P_c is computed by having data of close approach geometry between two objects involved as well as the uncertainty of the position knowledge. The result of the computation is a probabilistic assessment of the likelihood that the two objects will actually be at the same location at the same time.

A scale factor for this application is defined as the ratio between expected covariance today and expected covariance at solar maximum (around 2013). From Equations 5 and 6, it is shown that covariance can be expressed as a linear function of EDR. Therefore, the ratio of expected covariance is the same as the ratio of expected versus current EDR, which can be more easily predicted. The EDR values for 2010 and 2013 are lifted from Figure 7 for TRMM and Figure 8. The EDR ratio is formed as the quotient of these two values and is provided in Table 2.

Once the Covariance Scale Factors (from predicted versus current EDR ratio) are determined, the P_c can be re-computed using the scaled covariance and the effects of increased drag on P_c can be estimated. A Monte Carlo process simulated 5,000 conjunctions, by varying conjunction geometry. A covariance representative of today's solar flux activity was applied to each object to compute the P_c expected today. Then the covariance scale factors resulting from the EDR ratio from the nominal solar flux predictions as well as the EDR ratio from the +2 sigma solar flux predictions are applied and the P_c expected during high solar flux is computed.

Figure 9 shows scatter-plots of the P_c distribution for the simulated conjunctions in the TRMM orbit regime for (a) typical covariance today and (b) expected covariance during solar maximum. For these plots, a P_c less than 1E-10 is not shown as, operationally, these P_c values are assumed to be zero.

Table 2: Covariance Scale Factors Determined

Simulated Spacecraft	Nominal Solar Flux EDR Prediction Scale Factor Used	+2 Sigma Solar Flux EDR Prediction Scale Factor Used
Aqua	4.8	5.8
TRMM	3.2	3.2

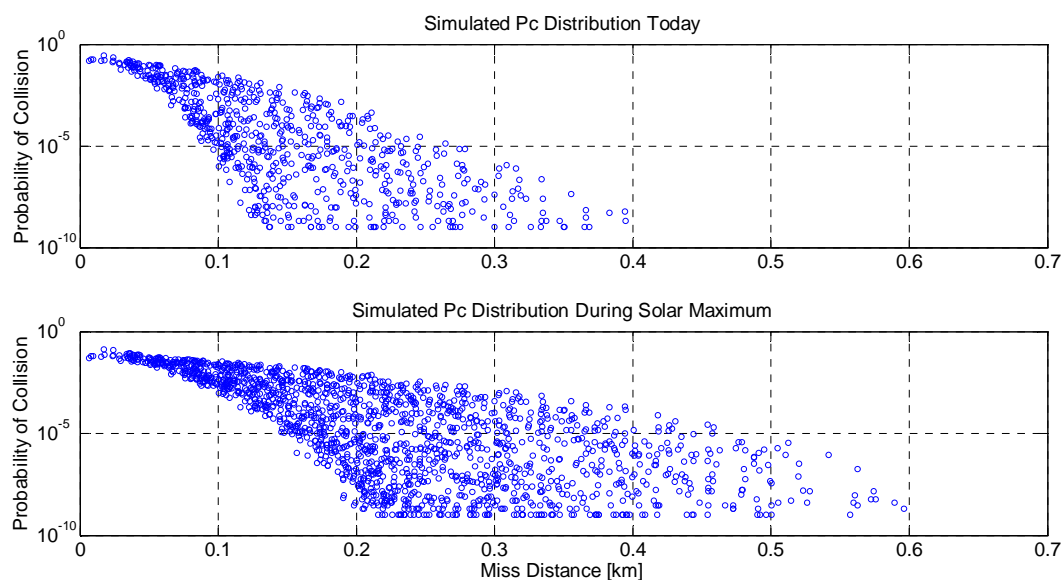


Figure 9: Difference in Computed Pc at 400 km for Nominal and +2 Sigma Solar Flux Predictions

The first major observation in Figure 9 is the distribution of Pc over miss distance. Specifically, with increased atmospheric drag effects on the covariance, higher probabilities are observed at larger miss distance. There are several $1\text{E-}5$ probability events at 250 meters today. However, during solar maximum $1\text{E-}5$ probabilities are observed to about 500 meters in 2013. Notionally, a $1\text{E-}5$ is a Pc for which at least additional analysis would be needed to determine the risk. Since the covariance scale factor determined for TRMM using the nominal and +2 sigma solar flux predictions was the same, this analysis was only performed once.

Figure 10 shows the results for a similar analysis for simulated conjunctions in the Aqua orbit regime. Similar effects of scaled covariance are observed at 700 km altitude. Events with probabilities greater than $1\text{E-}5$ are observed to about 100 meters in miss distance today, but up to 250 meters in 2013. The data in Figure 10 also shows that at extremely small miss distances, less the 25 meters, the probability observed today is higher than what will be expected during solar maximum. This is the opposite of what is observed at larger miss distances and is a direct consequence of the behavior described in Figure 2. At these small miss distance and with the covariances being considered, as the uncertainty increases the probability density function in the local area of the miss distance becomes less dense resulting in the lower Pc.

Figure 11 shows the probabilities for the Aqua regime using the +2 sigma solar flux estimate. The Aqua spacecraft operates at a significantly higher altitude than TRMM. As a result, the +2 sigma solar flux variation causes a more noticeable increase in drag at Aqua's altitude compared to TRMM as seen by the scale factors give in Table 2. It is expected that the increased scale factor would result in the Pc being more sensitive to the uncertainty in the solar flux prediction. Figure 11 shows that for the +2 sigma solar flux predictions, the increased scale factor only slightly increased the Pc values observed at larger miss distances compared to the mean profile. This suggests that for the solar flux predictions used in this analysis, the large scale change in mean flux over the 11 – year solar cycle is more significant than the uncertainty in the predicted mean profile.

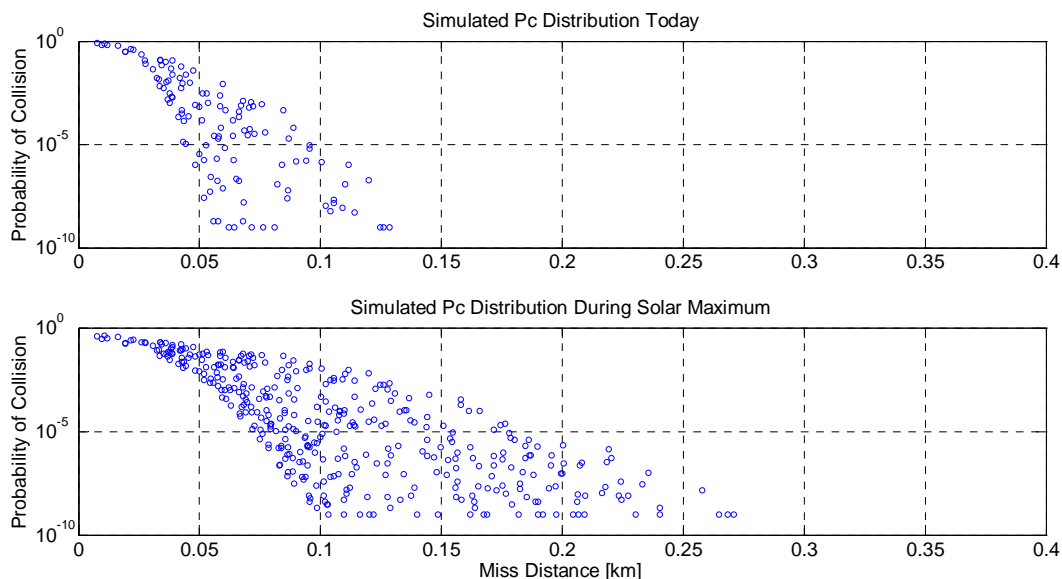


Figure 10: Difference in Computed Pc at 700 km for Nominal Solar Flux Predictions

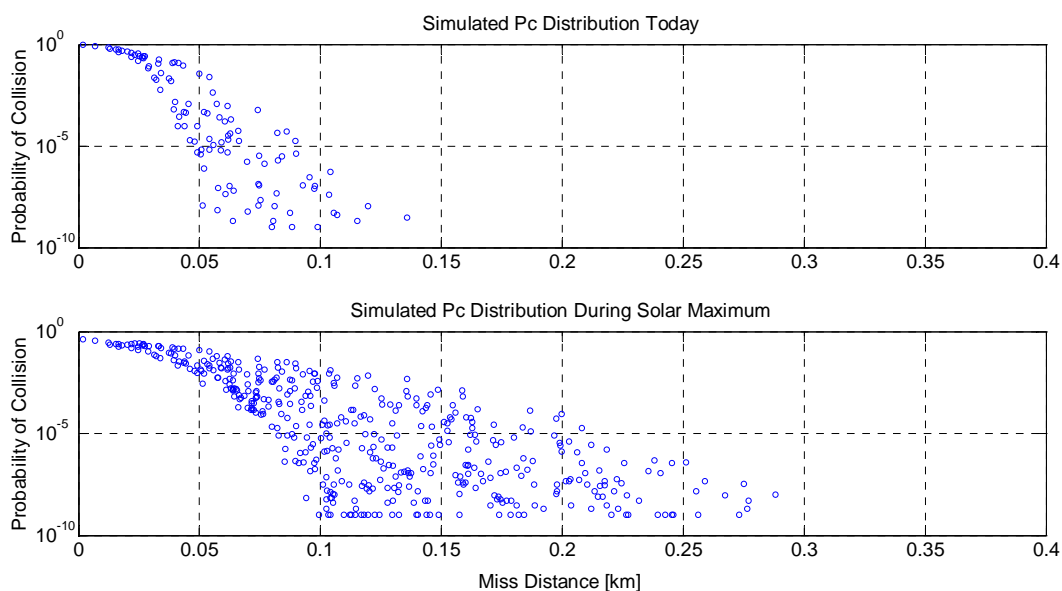


Figure 11: Difference in Computed Pc at 700 km for +2 Sigma Solar Flux Predictions

VI. Implications to Satellite Owner/Operators

This analysis has shown that as solar flux and drag increase through the next solar cycle, the uncertainty in orbit position knowledge will increase. The increases in uncertainty have been shown to have two impacts on the Pc. First, at extremely small miss distances, the Pc will tend to become smaller. Second, appreciable, actionable Pc will occur at greater miss distances. These results will lead to changes in actual risk mitigation operations.

Over the previous solar minimum, Owner/Operators (O/O) have become accustomed to the behavior of the Pc, essentially understanding that the most risky conjunctions will only occur at small miss distances. During the upcoming solar maximum, O/O will need to be ready to respond to conjunctions at larger miss distances.

Fortunately, for the data presented here, the miss distances of concern are still on the order of hundreds of meters. However, it should be noted that the upcoming solar cycle is expected to be relatively mild. For future solar cycles the drag environment may be significantly higher, resulting in high Pc at the kilometer level.

A more complicated situation potentially occurs at extremely small miss distances where the Pc may be lower during high drag environments. For extremely large covariance values, the Pc may even drop to zero at low miss distances. This presents a complicated risk analysis question. It may become difficult for O/O of high value assets to accept that objects coming within several tens of meters of their spacecraft do not present a risk, even if the Pc demonstrates this fact. Note that in this analysis we have accepted that the covariance accurately represents the state uncertainty. There are significant questions concerning covariance realism that are outside the scope of this paper. In these situations, depending on the O/O tolerance for risk, the best risk mitigation option may be to perform a maneuver that increases the miss distance significantly to completely eliminate the conjunction risk. The ability to perform such large maneuvers may be limited by fuel and/or other mission constraints.

The increase in covariance during solar maximum will also complicate the planning of risk mitigation maneuvers. The typical approach to mitigating a conjunction risk is to perform a maneuver that increases the miss distance to a point where the Pc vanishes. This typically happens when the miss distance is well outside of the 3-sigma combined uncertainty. Larger combined uncertainty will therefore require larger maneuvers. For a posigrade, in-plane, maneuver, the change in along track position of a spacecraft is given by [Reference 6]

$$\Delta I = -3\Delta v T \quad (7)$$

Where Δv is the applied change in velocity and T is the phasing time. The change in along track position can then drive the change in total miss distance for a conjunction. Given the data in Table 2, the covariance may be between five and six time those observed today, and therefore the required miss distance to mitigate conjunction risk will be five to six time larger. To achieve larger miss distances, risk mitigation maneuvers will require larger maneuvers and/or increase in phasing time, or time between the maneuver and the conjunction.

Typically, risk mitigation maneuvers are scheduled as close to the conjunction as possible to allow for improved orbit determination accuracies, so significantly increasing the phasing time may not be an option. Many missions, however, also have science driven orbit requirements, or propulsion system limitations that limit the delta-V that can be applied. For example, the Earth Science Constellation (ESC) missions Aqua, Aura, and Terra fly repeat ground track orbits that require them to maintain tight semi-major axis limits. These missions are also only normally limited to performing posigrade, in-plane maneuvers. Strategies for performing larger risk mitigation maneuvers will need to be developed for each missions unique orbit requirements and propulsion system limitations.

A final impact of increased covariance size is on the conjunction screening process. Conjunctions are identified by propagating space object states and finding when the distance between them is at a minimum. If the miss distance between the two objects meets certain criteria, the conjunction is reported and data produced to perform risk analysis. The geometry criteria are referred to as screening volumes. The screening volumes are typically elliptical or rectangular volumes in the asset spacecraft's Radial, In-Track, Cross Track (RIC) coordinate frame. The screening volume must be sized to identify all objects that may be a threat to the asset spacecraft.

For example, if spherical screening volume of 3 kilometer radius was used, and the typical combined covariance was on the order of 1 kilometer, the majority of risky conjunctions will be identified since the typical 3-sigma combined uncertainty falls within our screening volume. However, if the reverse scenario occurs and a 1 kilometer spherical screening volume is used, and the typical combined uncertainty is on the order of 3 kilometers, objects that fall outside of the 1 kilometer screening volume that are not identified will still have an appreciable Pc since the miss distance is less than the combined 3 – sigma error. Therefore, as the covariance size increases during the solar cycle, screening volumes sized to account for the expected combined uncertainty must be used when identifying conjunctions.

VII. Conclusions & Future Work

This paper has described an approach to determining the effects of increasing drag on conjunction assessment. Specifically, this analysis has presented a relationship between historical covariance and EDR, predicted EDR as a result of solar flux predictions, mapped EDR predictions to expected covariance, and observed these effects on Pc distribution for simulated conjunction events. The analysis shows that the hypothesis is correct in that spacecraft in LEO can expect, on average, to observe higher Probability of Collision computed for larger miss distance conjunctions. The increased expected EDR, covariance, and Pc distribution due to increased atmospheric drag is more prevalent at 700 kilometers LEO altitudes than at 400 kilometers.

There are several implications of the results of this analysis that deserve some comment. It has been shown that O/O should expect higher Probability of Collisions for larger miss distances compared to what they have grown accustomed. For simulated TRMM conjunctions at roughly 400 kilometers in altitude, the Pc using high drag scaling was observed for conjunctions with miss distance between 200-600 meters that was observed at 100-400 meters with no scaling for increased solar activity. Likewise, for simulate Aqua conjunctions at roughly 700 kilometers in altitude, the same Pc using covariance scaling at miss distances of 100-300 meters were observed at miss distances of 50-125 meters with no scaling. And this shift in Pc expectation has been shown to be purely a result of the increased solar activity affecting the atmospheric density in LEO. For TRMM, it is shown that covariance is sensitive to increases in solar activity but, during Solar Cycle #24, it is not sensitive to the expected or +2 sigma solar flux predictions; the upcoming solar cycle will affect covariance the same regardless of predicted solar maximum magnitude variations. For Aqua, on the other hand, covariance is more sensitive variations in solar activity for Solar Cycle #24.

Another way to state this finding is that the same conjunction geometry of concern today may not be of concern during heightened solar activity. Similarly, a conjunction that is not of concern today will be of concern during solar maximum. These resulting implications should be shared with O/O to promote awareness of the phenomenon. It is the view of the authors that true risk assessment comes only from a rigorous CARA process and fundamental understanding of the problem and not the result of one Pc computation. For missions that use the Pc as a metric for maneuver decisions, the results of this analysis has impacts on the number of maneuvers that might be performed.

Future analysis stemming from this study may include, but not limited to, examining future (and possibly more active) solar cycles, more LEO regimes, and parameterization of the covariance scale factoring methodology. Further characterization of the EDR to Covariance correlation will also be performed as more high drag data becomes available.

Acknowledgments

This paper was supported by NASA/GSFC, under the FDSS contract (NNG10CP02C), Task Order 21.

References

1. Newman, L. "The NASA Robotic Conjunction Assessment Process: Overview and Operation Experiences." Conference Proceedings. 59th International Astronautical Congress. 29 September – 3 October 2008. Glasgow, Scotland, United Kingdom. IAC-08-A.6.2.6.
2. Newman, Lauri Kraft, Frigm. R, McKinley, D. "It's Not a Big Sky After All: Justification for a Close Approach Prediction and Risk Assessment Process." Conference Proceedings. 2009 AIAA/AAS Astrodynamics Specialist Conference, 9-13 August 2009, Pittsburgh, PA. AAS 09-369.
3. Alfriend, K.T., Akella, M. R., Lee, D., Frisbee, J., Foster, J. L., "Probability of Collision Error Analysis," Space Debris Vol. 1, No. 1, Kluwer Academic Publishers, p. 21-35, 1999.
4. Schatten, K., "Fair Space Weather For Solar Cycle 24," Geophys. Res. Lett., 2005, 32, L21106-9.
5. Goddard Space Flight Center, "Flight Dynamics Facility Products Server," <https://wakata.nascom.nasa.gov/>, visited July 24, 2007.
6. McKinley, D. "Maneuver Planning for Conjunction Risk Mitigation with Groundtrack Control Requirements." Conference Proceedings. 18th AAS/AIAA Space Flight Mechanics Meeting. 27-31 January 2008. Galveston, TX. AAS 08-242.